

1 **Objective evaluation of ram and buck sperm motility by using novel sperm tracker software**

2 F. Buchelly Imbachí ^{1Ψ}, L. Zalazar ^{2 3Ψ}, J.I. Pastore ^{1 3}, M.B. Greco ^{2 3}, M. Iniesta-Cuerda ⁴, J.J.

3 Garde⁴, A.J. Soler ⁴, V. Ballarin ^{1*} and A. Cesari ^{2 3*}

4 ¹Laboratorio de Procesamiento de Imágenes ICYTE UNMDP – CONICET

5 ² Instituto de Investigaciones Biológicas IIB UNMDP – CONICET

6 ³ Consejo Nacional de Investigaciones Científicas y Técnicas CONICET

7 ⁴ Instituto de Investigación de Recursos Cinegéticos, Universidad de Castilla-La Mancha

8 (España)

9 ^Ψ Both authors equivalently contributed to the work from their disciplines

10 * Corresponding authors and equivalently directed the work from their disciplines

11

12 Running title: Novel open source software for sperm tracking

13 Keywords: Objective sperm motility, computer-assisted semen analysis system (CASA), sperm
14 kinetic parameters, open source tracking software, software performance evaluation.

15

16 Abstract

17 This work offers researchers the first version of an open-source sperm tracker software (Sperm
18 Motility Tracker V1.0) containing a novel suit of algorithms to analyze sperm motility using ram
19 and buck sperm as models. The computer-assisted semen analysis (CASA) is used in several
20 publications with increasing trend worldwide in the last years, showing the importance of
21 objective methodologies to evaluate semen quality. However, commercial systems are costly
22 and versatility is constrained. In the proposed method, segmentation is applied and the
23 tracking stage is performed by using individual Kalman filters and a simplified occlusion
24 handling method. The tracking performance in terms of precision (number of true tracks), the
25 percentage of fragmented paths and percentage of correctly detected particles were manually

26 validated by three experts and compared with the performance of a commercial motility
27 analyzer (Microptic's SCA®). The precision obtained with our Sperm Motility Tracker was
28 higher than the one obtained with a commercial software at the current acquisition frame rate
29 of 25 fps ($p < 0.0001$), concomitantly with a similar percentage of fragmented tracks
30 ($p = 0.0709$) at sperm concentrations ranging 25 and 37×10^6 cells/ml. Moreover, our tracker was
31 able to detect trajectories that were unseen by SCA®. Kinetic values obtained by using both
32 methods were contrasted. The higher values found were explained based on the better
33 performance of our sperm tracker to report speed parameters for very fast motile sperm. To
34 standardize results, acquisition conditions are suggested. This open-source sperm tracker
35 software has a good plasticity allowing researchers to upgrade according requirements and to
36 apply the tool for sperm from a variety of species.

37

38 Introduction

39 Motion analysis on quality assessment of semen samples is of great importance for the
40 positive association with male fertility and because it is in one of the most affected parameter
41 after cryopreservation. However, sperm tracking is quite complex due to cell collision,
42 occlusion and missed detection. Computer-assisted semen analysis (CASA) systems are used in
43 several publications with an increasing trend worldwide in the last years, showing the
44 importance of objective methodologies to evaluate semen quality and predict fertility. It is
45 well-known that CASA systems are commonly used for determination of sperm quality from
46 various species (Billard & Cosson 1992, Dietrich *et al.* 2005), cryopreservation effectiveness
47 (Cueto *et al.* 2016), toxicity bioassays, prediction of fertility potential or research related to
48 basic sperm biology (Muiño Otero 2008, Muiño 2008, Buzón Cuevas 2014).

49 CASA systems provide sequential digital images of each spermatozoa track allowing individual
50 motion analyzing thus facilitating a rapid, precise and accurate assessment of several and
51 meaningful kinetic measurements (Verstegen *et al.* 2002, Amann & Waberski 2014) that are

52 considered as objective and reproducible, while using identical instrument settings. On the
53 other hand, it has been recognized that among commercial software disadvantages, one can
54 mainly list high cost, need to regular upgrade and dramatic changes influenced by different
55 settings that are not well documented in publications (Schleh & Leoni 2013). Even when each
56 lab standardizes its own conditions, the setup of the parameters is crucial to allow
57 comparisons between different studies and to obtain reproducibility as well as consistency of
58 internal and external controls (Holt *et al.* 1994, Fraser 1998). Since there are many factors
59 affecting CASA performance (Broekhuijse *et al.* 2011), the methodologies and system
60 specificities (equipment, chamber, plate temperature and acquisitions details) have to be fully
61 and clearly described (Verstegen *et al.* 2002). However, these details are not often given in
62 most publications. Moreover, the accuracy of CASA results is intrinsically dependent of the
63 range of sperm concentrations analyzed (Muiño Otero 2008, Muiño 2008, Talarczyk-Desole *et*
64 *al.* 2017).

65 Another fact that has to be considered is that motility estimates and concentration using CASA
66 systems are highly influenced by the counting chamber (Hoogewijs *et al.* 2012, Palacín *et al.*
67 2013). Besides spermatozoa speeds vary according to each species, the choice of a particular
68 acquisition velocity is under discussion, since the selected frame rate affects the measure of
69 several kinetic parameters (Davis & Katz 1992, Verstegen *et al.* 2002). Verstegen *et al.* (2002)
70 described that trajectories are not well detected when setting of maximum velocity is too low,
71 in these cases the software generates wrong trajectories since it connects points belonging
72 from different spermatozoa tracks. In most of the cases, a good measure of a high curvilinear
73 velocity value is due to a good frame rate setting.

74 Concerning costs, there are also some open source systems that are widely useful in sperm
75 motility analysis, e.g. National Institutes of Health has developed a CASA plugin for the ImageJ
76 software (Wilson-Leedy & Ingermann 2011) that has been especially adapted for the kinetic
77 analysis of fish sperm (Verstegen *et al.* 2002) but also validated for mammalian sperm

78 (Giaretta *et al.* 2017). Disadvantages of this method include many manual settings, needing to
79 apply different thresholds to each video.

80 The aim of this work was to develop an automated particle detection tool and a suite of
81 tracking algorithms to analyze motility parameter characteristics using ram and buck sperm as
82 models. Our tool has the clear advantage that is plausible to be extrapolated to other species
83 due to its plasticity to perform changes depending on the researcher's objectives and the
84 intrinsic characteristics of the samples. Moreover, this prototype is useful to track each
85 spermatozoon since the corresponding trajectory is drawn step by step through the images
86 sequence.

87 In this way, we developed a sperm tracker software containing a suite of algorithms for sperm
88 motility analysis that includes the stages of detection (frame to frame), tracking and motility
89 analysis for videos of ram and buck sperm cells. A manual validation was performed to
90 compare the tracking performance of our algorithm with that of an available version of the
91 Microptic's Sperm Class Analyzer-SCA® over the same videos. This work offers an open-source
92 software to evaluate semen motility for researchers in the reproductive field

93

94 MATERIALS AND METHODS

95 Samples collection

96 Animal handling was performed in accordance with Spanish Animal Protection Regulation, RD
97 53/2013, which conforms to European Union Regulation 2010/63. Blanca Celtibérica buck and
98 Manchega ram (age > 1.5 years) were maintained in a semi-free ranging regime at El Campillo
99 (Elche de la Sierra, Albacete, Spain) or at experimental farm of University of Castilla-La
100 Mancha, respectively. The collection of ejaculates was performed using two different
101 methods: artificial vagina for ram (5 males) or electroejaculation for buck (5 males), according
102 to the guidelines RD 841/2011 and protocols previously described (Marco-Jimenez *et al.* 2008,

103 Jimenez-Rabadan *et al.* 2012). Ram samples were collected and pooled whereas samples from
104 buck were analyzed individually.

105 Sperm concentration was calculated by Bürker chamber counting and adjusted to 30×10^6
106 spermatozoa/ml for ram and 20×10^6 spermatozoa/ml for buck with a phosphate buffer (PBS)
107 at 37 °C.

108

109 Experimental procedure

110 Objective motility was assessed with a Makler® counting chamber (10 µm depth) and samples
111 were observed using a 10 X objective (negative phase contrast field). Each analysis captured
112 several fields with a Basler A302fs digital camera (Basler Vision Technologies, Ahrensburg,
113 Germany) connected to a computer by an IEEE 1394 interface. The image size was 768 x 576
114 pixels. The acquisition frame rate was set in 25 frames per second (fps) videos which were
115 simultaneously analyzed by Computer Assisted Semen Analysis (CASA) using the Sperm Class
116 Analyzer software (SCA® 2002, Microptic, Barcelona,Spain) and by our sperm motility tracker
117 software. Buck sperm tracking videos produced by our algorithm are available at Vimeo
118 homepage (see references <https://vimeo.com>) The motility parameters assessed are described
119 in section D (Motility Parameters and Motility analysis).

120

121 Algorithm development

122 A. Detection of the Cells Head

123 Image processing algorithms were developed in C++ with the Netbeans IDE and using the
124 OpenCV 3.2.0 library. A detection method similar to the one have been used by Buchelly *et al.*
125 (2016) for cells segmentation was used but with a highlighting step due to opening Top-Hat
126 (Serra 1982). For the Top-Hat transform we used a circular structuring element with the
127 sufficient size to enclose one spermatozoon head (11x11 pixels). The fixed threshold to obtain
128 the binary image was set to 30. The structuring element used for the binary morphological

129 filter is circle shaped and it has a size of 5 x 5 pixels to remove little noise points, sharp
 130 features like the sperm tails, and to separate some particles.

131

132 B. Concentration measurement

133 Cells concentration was determined for each sample video as the average number of cells in
 134 each frame per square millimeter (cells/cm³), according to (1):

$$135 \quad D = \left(10^8 \frac{\mu m}{cm^3} \frac{L^2}{d} \right) \left(\frac{\sum_{k=1}^N n_k}{w.h.N} \right) \quad (1)$$

136 Here, L and d are the setting parameters and depend on the experimental conditions: L is the
 137 length of the side of the gride square in pixels and d is the counting chamber depth in
 138 micrometers, w and h are the image width and height respectively in pixels. So, the first factor
 139 in (1) refers to the transformation of the lengths from pixels to metric units. By the other hand,
 140 the second factor shows the average number of cells in the video sequence determined by the
 141 numbers of cells in each frame (n_k) and the total number of frames, N .

142

143 C. Sperm cells tracking

144 In order to define an object's model, kinematic variables, shape or geometric descriptors,
 145 contours, gray levels or textures can be considered (Lucena López 2003, Azari *et al.* 2011, Liu *et*
 146 *al.* 2013, Jeong *et al.* 2014, Sahbani & Adiprawita 2016). From this set of data, the model is
 147 represented by the state X_i of the system at the instant i with a given number of degrees of
 148 freedom (Lucena López 2003). Our object's model consisted only on the head centroid or mass
 149 center coordinates (Gárate Polar 2015) and its velocity components. As it doesn't rely on the
 150 geometry of the cell head or on gray levels information, a spermatozoon was treated as a point
 151 particle. The dynamics of the system was studied with a first order model, i.e. positions and
 152 velocities are measured to predict the future positions. The trajectory of the j -the particle was
 153 defined as the discrete collection of positions at all the instants i . The velocity vector of a
 154 particle j between the instants $i-1$ and i , was determined using (2):

$$155 \quad V_{i,j} = (x_{i,j} - x_{i-1,j}, y_{i,j} - y_{i-1,j}) = (u_{i,j}, v_{i,j}) \quad (2)$$

156 The model of the dynamics offers an a priori distribution of probabilities about all the possible
 157 configurations of the current state of the system $p(X_i)$ having into account the estimated
 158 distributions for the previous instants $p(X_{i-1})$ to $P(X_{i-n})$. By the other hand, the temporal fusion
 159 method uses the Bayesian framework to integrate the a priori probabilities with the set of
 160 measures Z (coordinates of the centroids of the detected cells in the current frame) to find the
 161 a posteriori distribution (Lucena López 2003) given by (3):

$$162 \quad p(X_i|Z) \propto p(Z|X_i) \cdot p(X_i) \quad (3)$$

163 The objective was to maximize $p(X_i|Z)$ in order to estimate the new state (Lucena *et al.* 2010)
 164 or to give the correct labels to the new detected particles according to the previous known
 165 ones. In (3), the value $p(Z|X_i)$ is the observation model. Despite of its limitations, Kalman filter
 166 is ideal to use with Gaussian and unimodal distributions (Lucena López 2003), assuming
 167 constant or low acceleration rates (Vinaykumar & Jatoth 2014). We associated Kalman Filter to
 168 each detected particle to predict its future position (Catlin 1989, Azari *et al.* 2011, Jeong *et al.*
 169 2014), as follows: let the state of a single particle j at the instant i , and the measurement
 170 vector. The state and the measurement are estimated by using (4) and (5):

$$171 \quad X_{i,j} = A_j X_{i-1,j} + \varepsilon_j \quad (4)$$

$$172 \quad Z_{i,j} = H_j X_{i-1,j} + \delta_j \quad (5)$$

173 Where A_j is the transition matrix for the particle j and has the values shown in (6). By the other
 174 hand, H_j is the measurement matrix and for this work it corresponds to the identity matrix
 175 $I \in R^{4 \times 4}$; ε_j and δ_j ; and are vectors corresponding to the process noise and the measurement
 176 noise respectively. The noise vectors are initialized with a constant value and updated during
 177 the execution time.

$$178 \quad A_j = \begin{pmatrix} 1 & 0 & 1 & 0 \\ 0 & 1 & 0 & 1 \\ 0 & 0 & 1 & 0 \\ 0 & 0 & 0 & 1 \end{pmatrix} \quad (6)$$

179 We used the built-in functions included in the OpenCV library to create and use Kalman
 180 predictors. Each of them functions in a cyclic process that consists in three stages and each
 181 stage is complemented with a particular routine for our own purposes. First, the system
 182 obtains real measures of the state variables and compares them with the measures predicted
 183 by the Kalman filters in the previous iteration to do the association by a minimal distance
 184 criterion and thus get indirectly the maximization of the a posteriori distribution $p(X_{i,j}, Z_j)$ for
 185 each particle. The result of the first stage gives the cell path over which the motility analysis
 186 described in the following section is performed. In the second stage, the system gives to the
 187 Kalman predictors the new real data to correct the state $X_{i,j}$ and to update the error vectors ϵ_j
 188 and δ_j and the covariance matrices that are involved in the inner operations. At the third stage,
 189 Kalman filters predict the possible future location of each labeled particle by having its state in
 190 the current instant, i.e. finding the values of Z_j that maximize $p(Z_j | X_{i,j})$ and that is used in the
 191 first stage of the next iteration

192

193 D. Motility Parameters and Motility Analysis

194 Motility of each spermatozoon was defined by its current head velocity descriptors (Muiño
 195 Otero 2008, Muiño 2008, Buzón Cuevas 2014):

- 196 • Curvilinear Velocity (VCL): Velocity over the total distance moved in the path length,
 197 i.e., including all oscillations that occur in the head track. A ram spermatozoon is
 198 considered immotile if it has a curvilinear velocity less to $10 \mu\text{m/s}$, according to (7).
- 199 • Average Path Velocity (VAP): Velocity over a calculated, smoothed (low pass filtered)
 200 path, i.e., a shorter distance than that used for calculating VCL.
- 201 • Straight-Line Velocity (VSL): Velocity calculated using the straight-line (Euclidean)
 202 distance between the beginning and end of the sperm track.
- 203 • Amplitude of Lateral Head Displacement (ALH): The average value of amplitude of the
 204 oscillatory movement of the sperm head in each beat cycle.

- 205 • Beat Cross Frequency (BCF)-The frequency with which the actual track crosses the
 206 smoothed track (regardless of the oscillation direction).
- 207 • Straightness (STR, %): Measure of the oscillation of the curvilinear path with respect to
 208 the average trajectory, calculated as $VSL / VCL \times 100$. Indicates the straightness of the
 209 middle path.
- 210 • Linearity (LIN, %): Relationship between the straight-line velocity and the curvilinear
 211 velocity expressed as $VSL/VCL \times 100$
- 212 • Oscillation (WOB, %): It is a measure of the oscillation of the curvilinear trajectory with
 213 respect to the average trajectory, calculated as $VAP / VCL \times 100$.
- 214 • Total motility (%): percentage of sperm having a curvilinear velocity (VCL) > 10 $\mu\text{m} / \text{s}$.
- 215 • Progressive motility (MP, %): percentage of sperm presenting movement with a
 216 straightness index (STR) $\geq 80\%$ within the sample.
- 217 ○ Statics: $VCL < 10 \mu\text{m/s}$.
- 218 ○ Low progressive: $10 < VCL < 45 \mu\text{m/s}$.
- 219 ○ Mid progressive: $45 < VCL < 75 \mu\text{m/s}$.
- 220 ○ Rapid: $VCL > 75 \mu\text{m/s}$.

221 As described by other state of the art works (Rojas *et al.* 2012, Liu *et al.* 2013, Gárate Polar
 222 2015, Hidayatullah *et al.* 2015), the discrete set of positions for each spermatozoon head (j-th
 223 particle), VCL_j was obtained as the mean curvilinear velocity, as described by (7), using the
 224 notation defined in the previous sections:

$$225 \quad VCL_j = \frac{(8.1\mu\text{m}).Fr}{L(n_j-1)} \sum_{i=1}^{n_j-1} \sqrt{u_{i,j}^2 + v_{i,j}^2} \quad (7)$$

226

227 where Fr refers to the frame rate in frames per second, L is the side length of the grid square
 228 given in pixels used in (1), n_j is the number of points of the j-th particle path, $u_{i,j}$ and $v_{i,j}$ are
 229 the components of the velocity defined in (2), for the n_j-1 intervals.

230 VAP calculation depends on the particular method used for obtaining the smoothed path. Our
 231 proposed system uses the method mentioned in Hidayatullah et al. (2015) for smoothing the
 232 path and accordingly ALH and BCF parameters.

233

234 Manual validation

235 The variables considered were the number of total trajectories, the precision defined as the
 236 number of correct paths over total paths detected (8) and the percentage of fragmented
 237 trajectories.

238 Precision= $\frac{TP}{TP + FP}$

239 (8)

240
$$\frac{TP}{TP + FP}$$

241 Where TP represents the number of true positives or good tracks and FP is the number of false
 242 positives or wrongly assigned tracks. To classify a track as good or bad we used the criterion of
 243 three independent expert biologists that performed the manual validation for each path
 244 considering whether the labels were correctly conserved during occlusion states.

245 The percentage of correctly detected particles is defined as the number of detected sperm
 246 over the total particles labeled by each software according to the criteria of three experts.

247

248 Statistical analysis

249 Data were analyzed by GLMM (generalized linear mixed effect model) to determine statistical
 250 significance between both software (Zuur *et al.* 2009). Data associated to cell percentages
 251 were analyzed through models with binomial distribution, whereas the number of trajectories
 252 were analyzed by models with Poisson distribution. Velocities were analyzed with Gaussian
 253 error distribution. Normality of residuals was assessed by plotting theoretical quantiles versus
 254 standardized residuals (Q–Q plots). Homogeneity of variance was evaluated by plotting
 255 residuals versus fitted values. All analyses were performed using R software version 3.3.3

256 (RCoreTeam 2017), with the “lme4” package for Poisson and binomial models and the “nlme”
257 package for Gaussian models (Bates *et al.* 2015, Pinheiro *et al.* 2017). For all analyses,
258 statistical significant differences were determined at $p < 0.05$.

259

260 Sperm motility tracker software V 1.0

261 The software is free and an executable version will be provided upon request

262 (acesari@mdp.edu.ar). The software’s user interface provides a step-by-step guide for users.

263 Important instrumental considerations and settings for users are also included (Table 1).

264 Running times are suitable for standard laptop computers with i3 processor and at least 3 GB

265 of memory. Screen resolution can vary between 1280x800 and 1920x1080.

266 The input to our algorithm software is a sequence of time-lapse images currently encoded

267 either as an MP4, AVI or MOV video file of 5 s acquired at 25 fps. The output of the algorithm

268 is a database (.XLSX) containing the set velocity parameters, population parameters and sperm

269 concentration; a movie (.AVI) with the complete tracks and an image (.BMP) of the tracks.

270

271 Results

272 Particles firstly detected and localized with the highest possible accuracy were linked to form

273 particle trajectories. Detected particles had a near elliptical shape although their areas had a

274 low number of pixels (Fig. 1). The small size let us to approximate the spermatozoa heads as

275 point particles and not to consider their shapes as shown within the region in which we could

276 observe centroids detection (Figure 2). As shown, the intensity degradations avoided the

277 complete detection of the particles’ shape and thus, this supported the idea of working with

278 the point particle model. It was possible to measure sperm concentration by using (1), having a

279 range of particle concentrations between 12.64×10^6 cells/ml (38.83 cells/frame) and $42.29 \times$

280 10^6 cells/ml (129.92 cells/frame) for the considered samples (Table 2) consistent with sample

281 adjustment (Material and Methods, Sample collection).

282 In order to evaluate the tracking performance, the trajectories detected by our proposed
283 algorithm were compared to the ones found by Microptic's – SCA® for two kind of sperm
284 samples: buck and ram fresh ejaculates. A high percentage of the paths tracked by SCA were
285 also followed by our algorithm, and moreover the number of cells followed by the sperm
286 tracker software was higher than the one obtained with the SCA® motility software for both
287 kind of samples (Table 2), suggesting that several sperm particles were only tracked by our
288 method (Fig. 3). The percentage of tracked particles that do not correspond to spermatozoa
289 can vary depending on the quality of the sample, on how clean is the media or on the image
290 quality. In this case, the percentage of correctly detected particles of our proposed method
291 was even higher than the percentage for SCA (Table 2, $\chi^2= 489.61$, Df= 1, $p<0.0001$ for ram
292 and $\chi^2= 6.19$, Df= 1, $p=0.0128$ for buck). Even it is indeed an error, it must be considered as
293 possible and for this reason provided that the percentage of undesirable particles is low, both
294 software are equipped with a tool allowing manually curation or elimination of these labels.
295 Regarding the number of evaluated cells, i.e. those automatically detected and also visually
296 tracked by each expert; the proposed method was higher than the SCA® module for both
297 species ($\chi^2= 450.75$, Df= 1, $p<0.0001$ for ram samples and $\chi^2= 56.66$, Df= 1, $p<0.0001$ for buck
298 samples analysis, Table 2).

299 There are in the literature some measures that allow the performance evaluation for tracking
300 systems, but the ideal disparity test should be given by the comparison with a ground truth or
301 the point to point comparison of each instant for all the tracks, as done by Fang *et al.* (2017) ,
302 Philip *et al.* (2014) or Chau *et al.* (2004). Unfortunately, the SCA® module does not offer that
303 information to compare the differences between each path with the one obtained by our
304 proposed method. According to the criterion of the experts, trajectories were classified as
305 good or bad considering whether the labels were correctly conserved during occlusion states.
306 In this way, our system allows to identify and draw each sperm trajectory frame to frame,
307 representing an advantage over other commercial systems (see Sperm tracking videos). In

308 terms of performance, a 5 s video showing 120 cells/field acquired at 25 fps is enough to
309 produce a complete data sheet by this algorithm in 30 ms using a 1.3 GHz Intel Core i3
310 processor with 3 GB 1600 MHz DDR3 RAM. Precision and percentages of fragmented paths
311 were evaluated to compare each system through a manual tracking by three independent
312 experts (Table 2, Fig. 4). We showed that the performance of our method is similar to the one
313 measured for the Microptic's SCA® Motility module, with a better occlusion handling
314 evidenced by the higher precision ($\chi^2= 151.03$, Df= 1, $p<0.0001$, Fig. 4A) and a similar
315 percentage of fragmented ram sperm tracks ($\chi^2= 3.26$, Df= 1, $p=0.0709$, Fig. 4C). On the
316 contrary, for buck sperm samples, Microptic's SCA® Motility module showed better precision
317 and lower fragmented tracks than our method ($\chi^2= 16.99$, Df= 1, $p<0.0001$ and $\chi^2= 95.95$, Df=
318 1, $p<0.0001$ respectively, Fig. 4B and E). When the precision of each system or the percentage
319 of fragmented trajectories is plotted depending on the particles concentration, the better
320 precision of our algorithm can be observed at higher concentrations, while SCA® was more
321 successful for low concentrations ranges (Fig. 4C and F).

322 The dataset of kinetic values obtained by using both methods over the same ram recorded
323 samples showed that our method reported higher average speed values ($\chi^2= 592.53$, Df= 1,
324 $p<0.0001$ for VCL, $\chi^2= 118.19$, Df= 1, $p<0.0001$ for VSL and $\chi^2= 112.33$, Df= 1, $p<0.0001$ for
325 VAP, Fig. 5A), average AHL (amplitude of the lateral displacement of the head, $\chi^2= 102.55$, Df=
326 1, $p<0.0001$, Fig. 5B), BCF (wavelengths of the flagellar beat, $\chi^2= 157.09$, Df= 1, $p<0.0001$, Fig.
327 5B) and also a higher motile population ($\chi^2= 85.17$, Df= 1, $p<0.0001$, Fig. 5C) compared to
328 SCA® reports. Similar results were observed for these kinetic values when buck samples were
329 analyzed (Fig. 5 D-F, $\chi^2= 23.49$, Df= 1, $p=0.0004$ for VCL, $\chi^2= 12.81$, Df= 1, $p=0.0003$ for VSL,
330 $\chi^2= 17.55$, Df= 1, $p<0.0001$ for VAP, $\chi^2= 76.20$, Df= 1, $p<0.0001$ for BCF, $\chi^2= 6.39$, Df= 1,
331 $p=0.0115$ for ALH and $\chi^2= 18.52$, Df= 1, $p<0.0001$ for total motility). Manual validation showed
332 that SCA® failed in tracking and reporting sperm with very high speeds often rendering in non-
333 detected cells (e.g., sperm indicated with yellow arrows in Fig. 3) or otherwise fragmenting the

334 trajectories with low speed assigned to a little stretch (e.g., sperm indicated with yellow
335 arrows in Fig. 6). Accordingly, the report of kinetic values obtained by using both methods over
336 the same cells (i.e. cells tracked by both softwares) showed comparable values (Fig. 6, green
337 arrows). Consequently, differences can be explained on the basis of the better performance of
338 our sperm tracker to report speed parameters for very fast motile sperm and to the increment
339 in the number of tracks (Table 2) mainly corresponding to motile spermatozoa (Fig. 5C and F).

340

341 Discussion

342

343 In this work, we presented a new detection and tracking algorithm that can effectively identify
344 immotile as well as motile and progressive sperm heads from two different species, with
345 different concentration ranges and bearing different proportions of motile sperm. We
346 demonstrated that the proposed approach can successfully handle challenges such as cell
347 collision and occlusion, succeeding in multiple sperm tracking, when the spermatozoa
348 concentration up to 42.29×10^6 cells/ml. Our free access tool was validated against CASA
349 SCA[®], providing similar values of sperm parameters but was more efficient in the number and
350 precision of detected tracks at high concentration ranges, as well as in relation to the lower
351 number of fragmented trajectories.

352 Some single particle tracking algorithms have been developed, however they mostly failed in
353 following them simultaneously when more than 10 cells co-exist (Imani *et al.* 2014, Tinevez *et*
354 *al.* 2017). Recently, an automated multi-sperm tracking algorithm capable to detect and track
355 simultaneously hundreds of human sperm cells from two samples was presented with the
356 limitations of long time required to process each video at low acquisition speed and lack of
357 validation against a standardized method (Urbano *et al.* 2017).

358 Many cells segmentation methods have been proposed in literature for microscopy image
359 sequences. Some works first binarize the images and others use a matching template.

360 Hidayatullah *et al.* (2015), Gárate Polar (2015) and Rojas *et al.* (2012) proposed a fixed
361 threshold and then a binary morphological filter; Buchelly *et al.* (2016) applied a mathematical
362 morphology gray filter to highlight sperm heads and a later threshold; Liu *et al.* (2013) ,
363 Vinaykumar and Jatoth (2014) applied temporal frame differencing, a fixed threshold and a
364 binary morphological filter and others use background subtraction, thresholding and binary
365 filtering (Azari *et al.* 2011, Jeong *et al.* 2014). Other approaches also exist that use
366 simultaneous detection and tracking with their own considerations (Karthikeyan *et al.* 2012,
367 Boryshpolets *et al.* 2013).

368 It is consensus that standardization is needed to avoid variations in semen analysis (Palacín *et*
369 *al.* 2013). One of the most important settings of the assay is cell concentration. In this sense,
370 Wilson-leedy and Ingermann (2007) have studied the effect of the cells concentration upon
371 motility measurements, as well as we do, finding that the main limitation is particle density.
372 The widest dynamic range allowed the higher plasticity of the tool, which is critical when
373 considering working with sperm from different species For example, the VCL range for ram
374 motile sperm is between 189.8 ± 40.7 and 39.8 ± 21.0 $\mu\text{m/s}$ (Ledesma *et al.* 2017), while for
375 fish the VCL range is between 330 ± 70 and 20 ± 15.0 $\mu\text{m/s}$ for a variety of species (Fauvel *et al.*
376 2010, Fabbrocini *et al.* 2016). This is an advantage when compared to commercial systems that
377 are specie-specific. On the other hand, there should be some other adjustments needed for
378 correct sperm identification in other species associated to differences in sperm morphology
379 and size.

380 According to Lucena (2003), a typical tracking scheme has four basic essential elements: image
381 features, model of the objects, model of the dynamics, and a temporal fusion method. The
382 most of the works in the state of the art use intensity distribution (Karthikeyan *et al.* 2012,
383 Rojas *et al.* 2012, Jeong *et al.* 2014, Gárate Polar 2015, Hidayatullah *et al.* 2015); however
384 there also exist more features that can be used like color (Lucena *et al.* 2010, Fang *et al.* 2017),
385 motion history (Liu *et al.* 2013), optical flow (Lucena *et al.* 2015), frequency descriptors (Pei *et*

386 *al.* 2006), and others. As mentioned before, we used the intensity distribution as the image
387 feature required to detect the spatial distribution of cells at each instant, because of the high
388 contrast obtained between foreground and background in the scene.

389 A common trouble in tracking systems is the occlusions handling. In this situation, two or more
390 objects in the 2D scene get very close to each other and the detection module often considers
391 them as a single object, giving to the system the ambiguity of which label corresponds to this
392 new object and how to treat the absence of the missing others. The tracking scheme must lead
393 with this situation and take a proper decision. The method (Azari *et al.* 2011) applied template
394 matching in the region of occlusion and used correlation to identify the parts corresponding to
395 each merging individual object. In Jeong *et al.* (2014) the aspect ratio or width/height is
396 considered to detect when object are merging or splitting. In Lucena *et al.* (2010), authors use
397 a combined model of the mean-shift and the CAM-Shift algorithms to improve robustness to
398 occlusion. The occlusion handler of Sahbani and Adiprawita (2016) uses the statistics of the
399 blob size (standard deviation) to find an occlusion situation by means of an occlusion
400 threshold. When an occlusion condition occurs due to merging objects, the label of the new
401 particle corresponds to the label of the previous object that presented the closer prediction
402 point to the measured mass center. Meanwhile, the position of the hidden object is predicted
403 during a test interval of 6 frames with an increasing search radius. Then, if the particle appears
404 during the test interval and inside the search region, it will recover its original label and its path
405 will be completed with the previous estimated locations.

406 Many similar works have developed solutions to make an automatic motility analysis, both for
407 human and other animals' sperm. In this work, we take the known methods to determine the
408 motility parameters and own considerations, but we put our major interest in the system
409 performance evaluation. An important fact to consider is the objectivity of the curvilinear
410 velocity (VCL) measurement and the subjectivity of the average path velocity (VAP). The VAP
411 parameter depends of the smoothness degree of the spermatozoon trajectory and there is no

412 information about a unified criterion to perform that low pass filtering operation and, in
413 consequence, each system performs it in a different way giving probably different results for
414 the same sample video. The subjectivity in the method to measure the VAP parameter also
415 carries subjectivity in measuring the other ones that depends on it: Amplitude of Lateral Head
416 Displacement (ALH) and Beat Cross Frequency (BCF).

417 By the other hand, the VAP calculation depends on the particular method used for obtaining
418 the smoothed path. In Hidayatullah et al. (2015), authors showed the implementation of a
419 moving average filter with a fixed size of 5 elements. Rojas *et al.* (2012) used an approximation
420 based on the Bezier Plane method. Wilson-Leedy and Ingermann (2007) used a moving
421 average filter which size depends on the frame rate. The Microptic's - SCA® establishes VAP as
422 one of the modifiable parameters by the user and thus makes it more inter subjective.

423 Sperm kinetic parameters determined by our software compared with the values offered by
424 the reference software (Microptic's - SCA®) over the same samples were able to get
425 comparable output data when measuring the same sperm particles. However due to the
426 better performance of our software to correctly track high speed sperm, a higher percentage
427 of rapid sperm and consequently average higher speed values were reported by our algorithm.

428 It is important to consider that the measure of VSL depends only on the final and initial points
429 of each path, so it could be directly validated by the tracking performance. Moreover, for
430 different samples and laboratories comparisons between available CASA systems should be
431 carefully done since several factors inherent to motility acquisition settings affect the
432 standardization. The other parameters (VAP, ALH, BCF) depend on which smooth filter was
433 applied to the original path and currently there is no standardized criterion to select one as the
434 best choice, as mentioned before.

435 Finally, whereas most of the studies conducted nowadays to boost standardization of sperm
436 motility assessment systems are focused on the software capacities, in this study we also
437 analyze the equipment requirements. It is known that commercial systems have been

438 improving their software and also associated cameras according to users' demand. However,
 439 in the research field labs acquire commercial CASA systems that cannot be often modernized
 440 and furthermore, publications are based on available equipment. In this sense, the choice of
 441 the velocity parameter describing the motility also depends on the video camera used.
 442 According to Wilson-leedy and Ingermann (2007) , low speed recording will hide the
 443 modifications of tracks during large time intervals (1/25 s for example) so that VCL and VAP
 444 would be quite similar. Our tool can be adapted to a range of acquisition speed (fps),
 445 suggesting that the tracking system could manage different number of frames in the same
 446 time lapse. This is particularly useful for species with high speed sperm, complex trajectories
 447 or unusual head/flagella movements.
 448 As a conclusion, this work presented new an-open-source sperm tracker software to sperm
 449 motility analyze at a range of different cell concentrations, taking ram and buck sperm as
 450 models. The tool has the possibility to be adapted by the creators to any other sperm species.

451

452 **Declaration of interest**

453 The authors have nothing to disclose.

454

455 **Funding**

456 This research was supported by National Agency for Scientific and Technological Promotion
 457 (ANPCyT, PICT-2015-3682) and National Scientific and Technical Research Council (CONICET,
 458 Argentina, PIP 2014-0273) grants.

459

460 **References**

- 461 **Amann RP & Waberski D** 2014 Computer-assisted sperm analysis (CASA): capabilities and
 462 potential developments. *Theriogenology* **81** 5-17 e11-13.
 463 **Azari M, Seyfi A & Rezaie AH** 2011 Real Time Multiple Object Tracking and Occlusion
 464 Reasoning Using Adaptive Kalman Filters. In *7th Iranian Machine Vision and Image*
 465 *Processing (MVIP)*, pp. 1-5.

- 466 **Bates D, Mächler M, Bolker B & Walker S** 2015 Fitting linear mixed-effects models using lme4.
467 *Statistical Software* **67** 1-48.
- 468 **Billard R & Cosson MP** 1992 Some Problems Related To the Assessment of Sperm Motility in
469 Fresh-Water Fish. *Journal of Experimental Zoology* **261** 122-131.
- 470 **Boryshpolets S, Kowalski RK, Dietrich GJ, Dzyuba B & Ciereszko A** 2013 Different computer-
471 assisted sperm analysis (CASA) systems highly influence sperm motility parameters.
472 *Theriogenology* **80** 758-765.
- 473 **Broekhuijse MLWJ, Šoštarić E, Feitsma H & Gadella BM** 2011 Additional value of computer
474 assisted semen analysis (CASA) compared to conventional motility assessments in pig
475 artificial insemination. *Theriogenology* **76** 1473-1486.
- 476 **Buchelly F, Pedetta A, Pastore J, Herrera K & Ballarin V** 2016 Automatic tracking of flagellar
477 rotation of bacteria. In *VII Congreso Latinoamericano de Ingeniería Biomédica (CLAIB)*,
478 pp. 46 (<http://www.abioin.com/pdf/cartilla.pdf>)
- 479 **Buzón Cuevas A** 2014 Análisis cinético y morfológico del espermatozoide del caballo
480 empleando el sistema Sperm Class Analyzer. In *University of Cordoba, Spain*, pp. 172.
- 481 **Catlin DE** 1989 Estimation, Control, and the Discrete Kalman Filter. *Applied Mathematical*
482 *Sciences* **71**. New York: Springer-Verlag, pp. 285.
- 483 **Cueto M, Gibbons A, Bruno M & Fernández J** 2016 Manual de obtención, procesamiento y
484 conservación del semen ovino, pp. 22.
- 485 **Davis RO & Katz DF** 1992 Standardization and comparability of CASA instruments. *Journal of*
486 *Andrology* **13** 81-86.
- 487 **Dietrich GJ, Kowalski R, Wojtczak M, Dobosz S, Goryczko K & Ciereszko A** 2005 Motility
488 parameters of rainbow trout (*Oncorhynchus mykiss*) spermatozoa in relation to
489 sequential collection of milt, time of post-mortem storage and anesthesia. *Fish*
490 *Physiology and Biochemistry* **31** 1-9.
- 491 **Fabbrocini A, D'Adamo R, Del Prete F, Maurizio D, Specchiulli A, Oliveira LF, Silvestri F &**
492 **Sansone G** 2016 The sperm motility pattern in ecotoxicological tests. The CRYO-
493 Ecotest as a case study. *Ecotoxicol Environ Saf* **123** 53-59.
- 494 **Fang Y, Yuan Y & Li L** 2017 Performance Evaluation of Visual Tracking Algorithms on Video
495 Sequences With Quality Degradation. *IEEE Access* **5** 2430 - 2441.
- 496 **Fauvel C, Suquet M & Cosson J** 2010 Evaluation of fish sperm quality. *Journal of Applied*
497 *Ichthyology* **26** 636-643.
- 498 **Fraser L** 1998 Guidelines on the application of CASA technology in the analysis of spermatozoa.
499 ESHRE Andrology Special Interest Group. European Society for Human Reproduction
500 and Embryology. *Human reproduction (Oxford, England)* **13** 142-145.
- 501 **Gárate Polar DA** 2015 Modelo heurístico para la determinación de la motilidad en células
502 espermáticas mediante el análisis automático de tracking en video. In *Pontificia*
503 *Universidad Católica del Perú*, pp. 40.
- 504 **Giaretta E, Munerato M, Yeste M, Galeati G, Spinaci M, Tamanini C, Mari G & Bucci D** 2017
505 Implementing an open-access CASA software for the assessment of stallion sperm
506 motility: Relationship with other sperm quality parameters. *Anim Reprod Sci* **176** 11-
507 19.
- 508 **Hidayatullah P, Awaludin I, Kusumo RD & Nuriyadi M** 2015 Automatic sperm motility
509 measurement. In *Information Technology Systems and Innovation (ICITSI), 2015*
510 *International Conference on*, pp. 1-5.
- 511 **Holt W, Watson P, Curry M & Holt C** 1994 Reproducibility of computer-aided semen analysis:
512 comparison of five different systems used in a practical workshop. *Fertility and sterility*
513 **62** 1277-1282.
- 514 **Hoogewijs M, De Vlieghe S, Govaere J, De Schauwer C, de Kruif A & Van Soom A** 2012
515 Influence of counting chamber type on CASA outcomes of equine semen analysis.
516 *Equine veterinary journal* **44** 542-549.

- 517 <https://vimeo.com/264473468>, <https://vimeo.com/264473359>,
518 <https://vimeo.com/264473293>, <https://vimeo.com/264473195>,
519 <https://vimeo.com/264473092>, <https://vimeo.com/264472125>,
520 <https://vimeo.com/264472024>, <https://vimeo.com/264471893>,
521 <https://vimeo.com/264471098>, <https://vimeo.com/264470218> whereas ram sperm
522 tracking videos at: <https://vimeo.com/265053190>, <https://vimeo.com/264482322>,
523 <https://vimeo.com/264482904>, <https://vimeo.com/264483470>,
524 <https://vimeo.com/264485794>, <https://vimeo.com/265054082>,
525 <https://vimeo.com/265055033>, <https://vimeo.com/265055885>,
526 <https://vimeo.com/265056710>, <https://vimeo.com/264487378>).
- 527 **Imani Y, Teyfour N, Ahmadzadeh MR & Golabbakhsh M** 2014 A new method for multiple
528 sperm cells tracking. *Journal of medical signals and sensors* **4** 35.
- 529 **Jeong J-m, Yoon T-s & Park J-b** 2014 Kalman Filter Based Multiple Objects Detection-Tracking
530 Algorithm Robust to Occlusion. In *SICE Annual Conference 2014*, pp. 941-946.
- 531 **Jimenez-Rabadan P, Ramon M, Garcia-Alvarez O, Maroto-Morales A, del Olmo E, Perez-**
532 **Guzman MD, Bisbal A, Fernandez-Santos MR, Garde JJ & Soler AJ** 2012 Effect of
533 semen collection method (artificial vagina vs. electroejaculation), extender and
534 centrifugation on post-thaw sperm quality of Blanca-Celtiberica buck ejaculates. *Anim*
535 *Reprod Sci* **132** 88-95.
- 536 **Karthikeyan S, Delibaltov D & Gaur U** 2012 Unified probabilistic framework for simultaneous
537 detection and tracking of multiple objects with application to bio-image sequences. In
538 *19th IEEE International Conference on Image Processing (ICIP)*, pp. 1349-1352.
- 539 **Ledesma A, Zalazar L, Fernández-Alegre E, Hozbor F, Cesari A & Martínez-Pastor F** 2017
540 Seminal plasma proteins modify the distribution of sperm subpopulations in
541 cryopreserved semen of rams with lesser fertility. *Anim Reprod Sci* **184** 44-50.
- 542 **Liu J, Leung C, Lu Z & Sun Y** 2013 Quantitative analysis of locomotive behavior of human sperm
543 head and tail. *IEEE Transactions on Biomedical Engineering* **60** 390-396.
- 544 **Lucena López MJ** 2003 Uso del flujo óptico en algoritmos probabilísticos de seguimiento. Tesis
545 Doctoral. In *University of Jaén, Informatic Department*
546 (file:///C:/Users/andre/Downloads/66.pdf)
- 547 **Lucena M, Fuertes JM & de la Blanca NP** 2015 Optical flow-based observation models for
548 particle filter tracking. *Pattern Analysis and Applications* **18** 135-143.
- 549 **Lucena M, Fuertes JM, De La Blanca NP & Marín-Jiménez MJ** 2010 Tracking people in video
550 sequences using multiple models. *Multimedia Tools and Applications* **49** 371-403.
- 551 **Marco-Jimenez F, Vicente JS & Viudes-de-Castro MP** 2008 Seminal plasma composition from
552 ejaculates collected by artificial vagina and electroejaculation in Guirra ram. *Reprod*
553 *Domest Anim* **43** 403-408.
- 554 **Muiño Otero R** 2008 Evaluación de la motilidad y viabilidad del semen bovino mediante el uso
555 de sistemas casa y citometría de flujo: identificación de subpoblaciones espermáticas.
556 In *Patología Animal*, pp. 354.
- 557 **Palacín I, Vicente-Fiel S, Santolaria P & Yániz J** 2013 Standardization of CASA sperm motility
558 assessment in the ram. *Small ruminant research* **112** 128-135.
- 559 **Pei S-c, Kuo W-y & Huang W-t** 2006 Tracking Moving Objects in Image Sequences Using 1-D
560 Trajectory Filter. *IEEE Signal Processing Letters* **13** 13-16.
- 561 **Philip RC, Ram S, Gao X & Rodr JJ** 2014 A Comparison of Tracking Algorithm Performance for
562 Objects in Wide Area Imagery. In *Image Analysis and Interpretation (SSIAI), 2014 IEEE*
563 *Southwest Symposium on*, pp. 109-112.
- 564 **Pinheiro J, Bates D, DebRoy S & Sarkar D** 2017 nlme: Linear and Nonlinear Mixed Effects
565 Models. R package version 3.1-131.
- 566 **RCoreTeam** 2017 R: A Language and Environment for Statistical Computing. R Core Team. R
567 Foundation for Statistical Computing, Vienna, Austria. URL [http://www.R-](http://www.R-project.org/)
568 [project.org/](http://www.R-project.org/).

- 569 **Rojas HA, Rojas JA, Zuleta GA & Madrigal CA** 2012 Extraction of new features for classification
570 of porcine sperm motility. In *17th Symposium of Image, Signal Processing, and*
571 *Artificial Vision*, pp. 323-327.
- 572 **Sahbani B & Adiprawita W** 2016 Kalman Filter and Iterative-Hungarian Algorithm
573 Implementation for Low Complexity Point Tracking as Part of Fast Multiple Object
574 Tracking System. In *6th International Conference on System Engineering and*
575 *Technology (ICSET)*, pp. 109-115.
- 576 **Schleh C & Leoni AL** 2013 How to optimize the benefits of computer assisted sperm analysis in
577 experimental toxicology. *J Occup Med Toxicol* **8** 6.
- 578 **Serra J** 1982 Image Analysis and Mathematical Morphology. 630.
- 579 **Talarczyk-Desole J, Berger A, Taszarek-Hauke G, Hauke J, Pawelczyk L & Jedrzejczak P** 2017
580 Manual vs. computer-assisted sperm analysis: can CASA replace manual assessment of
581 human semen in clinical practice? *Ginekologia Polska* **88** 56-60.
- 582 **Tinevez J-Y, Perry N, Schindelin J, Hoopes GM, Reynolds GD, Laplantine E, Bednarek SY,**
583 **Shorte SL & Eliceiri KW** 2017 TrackMate: An open and extensible platform for single-
584 particle tracking. *Methods* **115** 80-90.
- 585 **Urbano LF, Masson P, VerMilyea M & Kam M** 2017 Automatic Tracking and Motility Analysis
586 of Human Sperm in Time-Lapse Images. *IEEE Trans Med Imaging* **36** 792-801.
- 587 **Verstegen J, Iguer-Ouada M & Onclin K** 2002 Computer assisted semen analyzers in andrology
588 research and veterinary practice. *Theriogenology* **57** 149-179.
- 589 **Vinaykumar M & Jatoth RK** 2014 Performance Evaluation of Alpha-Beta and Kalman Filter for
590 Object Tracking. In *International Conference on Advanced Communication Control and*
591 *Computing Technologies*, pp. 1369-1373.
- 592 **Wilson-Leedy J & Ingermann R** 2011 Computer assisted sperm analysis using ImageJ;
593 description of necessary components and use of free software
594 (<https://imagej.nih.gov/ij/plugins/docs/CASAIstructions.pdf>).
- 595 **Wilson-Leedy JG & Ingermann RL** 2007 Development of a novel CASA system based on open
596 source software for characterization of zebrafish sperm motility parameters.
597 *Theriogenology* **67** 661-672.
- 598 **Zuur AF, Leno EN, Walker N, Saveliev AA & Smith GM** 2009 *Mixed Effects Models and*
599 *Extensions in Ecology with R* New York: Springer, Verlag New York, pp. 574.
- 600

601

602

603 **Legends and Tables**

604

605 **Sperm tracking videos.** Each line indicates the spermatozoa tracked by our sperm tracker

606 software frame to frame. Numbers identify each spermatozoa. Different colors of paths

607 indicate the different sperm velocities (static, low, medium or rapid sperm).

608

609

610 **Figure 1: Signal processing for the detection process. Upper panel,** a region of interest in a611 sample frame is selected to explain the detection process. **Lower panel,** Top-Hat

612 transformation of the selected area (left), binary image obtained by applying a fixed threshold

613 (center), and binary morphological opening to obtain only the heads(right). Bar= 25 μm .

614

615 **Figure 2: Zoom of a region with detected spermatozoa heads and their centroids.** Bar= 10616 μm .

617

618

619 **Figure 3: Visual comparison between trajectories detected by the SCA® versus the**620 **trajectories detected by the purposed sperm tracker software.** The images correspond to the621 same video acquired at 25 fps (Video 5 of Table 2, <https://vimeo.com/264485794>), showing622 the totality of paths detected by the SCA® module (**upper panel**) or our tracker software623 (**lower panel**). Bar= 25 μm . Curvilinear Velocity (VCL, $\mu\text{m/s}$) of some sperm that were not

624 detected with SCA® software (yellow arrows) are indicated with labels and arrows in the

625 bottom panel corresponding to our software.

626

627 **Figure 4: Performance of the sperm tracker software.** Percentage of fragmented paths (**A, B**
 628 **and C**) or precision (**D, E and F**) for our Sperm tracker system (SMT software) compared to
 629 SCA® (SCA software) at 25 fps. Ram (A and D) or buck (B and E) sperm were analyzed. **C and F**
 630 **panels** gather results of all the analysis consider cell concentration as a variable. Data
 631 assemble the reports of three independent experts that analyzed 10 videos for each species. *
 632 Value significantly different with respect to SCA® software ($p < 0.05$).

633

634 **Figure 5: Report of Kinetic parameters analyzed by the commercial CASA system (SCA®) and**
 635 **the sperm motility tracker software (SMT) purposed by us.** Sperm velocities: VAP, VSL and
 636 VCL (**A and D**), ALH and BCF (**B and E**) as well as total motility (**C and F**) were analyzed by both
 637 methods (SCA and SMT software) over the same samples. Analysis of ram samples are shown
 638 in A-C whereas analysis of buck samples are shown in D-E. . * Value significantly different with
 639 respect to SCA® software ($p < 0.05$). VAP: Average Path Velocity, VSL: Straight-Line Velocity,
 640 VCL: Curvilinear Velocity, ALH: Amplitude of Lateral Head Displacement, BCF: Beat Cross
 641 Frequency.

642

643 **Figure 6: Visual comparison between trajectories detected by the SCA® (upper panel) versus**
 644 **the trajectories detected by the purposed sperm tracker software (bottom panel).** The
 645 images correspond to the same video (Video 2 of Table 2, <https://vimeo.com/264482322>)
 646 acquired with 25 fps, showing the totality of paths detected with the SCA® module (upper
 647 panel) and our tracker software (bottom panel). Bar= 25 μm . Curvilinear Velocities (VCL, $\mu\text{m/s}$)
 648 of some paths fragmented by SCA® software but tracked correctly by SMT are indicated with
 649 labels (1-9) and yellow arrows in the corresponding panels. Tracks with similar VCL ($\mu\text{m/s}$)
 650 comparing SMT to SCA® are indicated with labels (10-13) and green arrows in the
 651 corresponding panels.

652

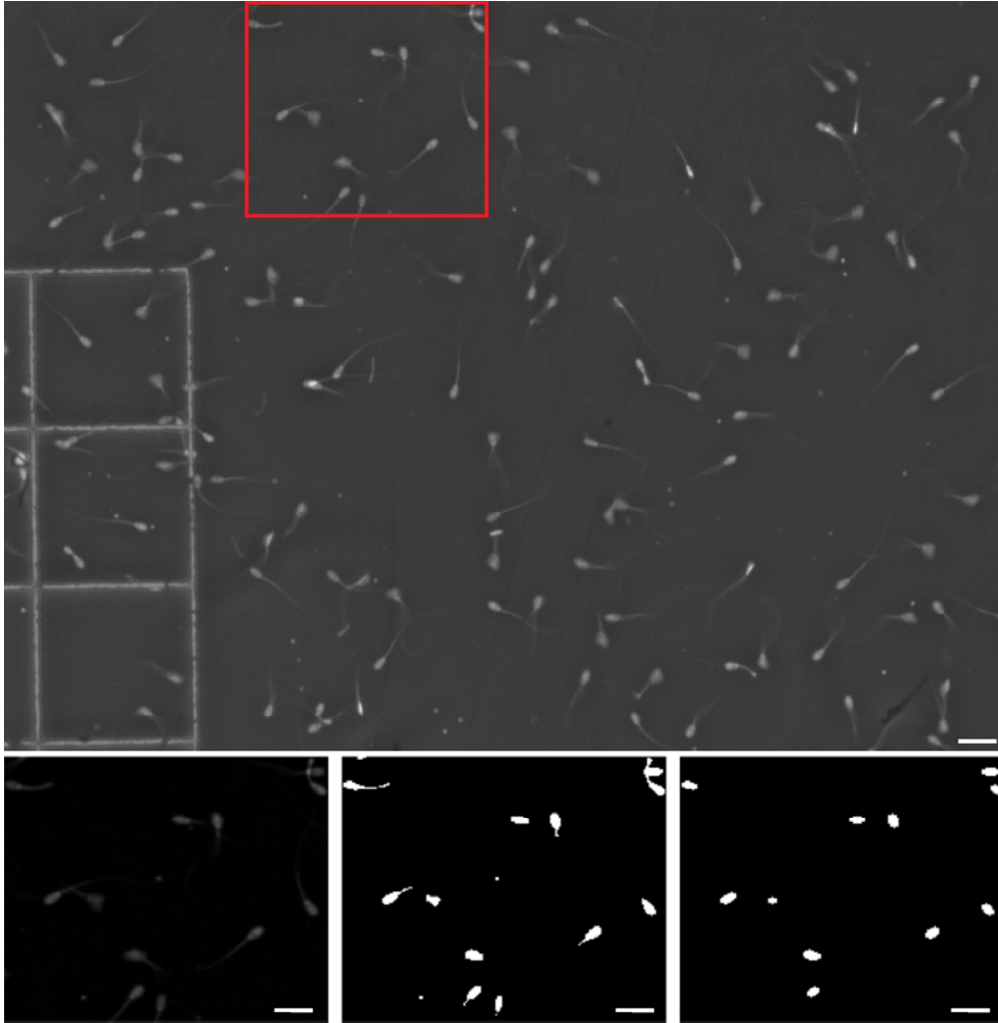


Figure 1: Signal processing for the detection process. Upper panel, a region of interest in a sample frame is selected to explain the detection process. Lower panel, Top-Hat transformation of the selected area (left), binary image obtained by applying a fixed threshold (center), and binary morphological opening to obtain only the heads(right). Bar= 25 μ m.

85x86mm (300 x 300 DPI)

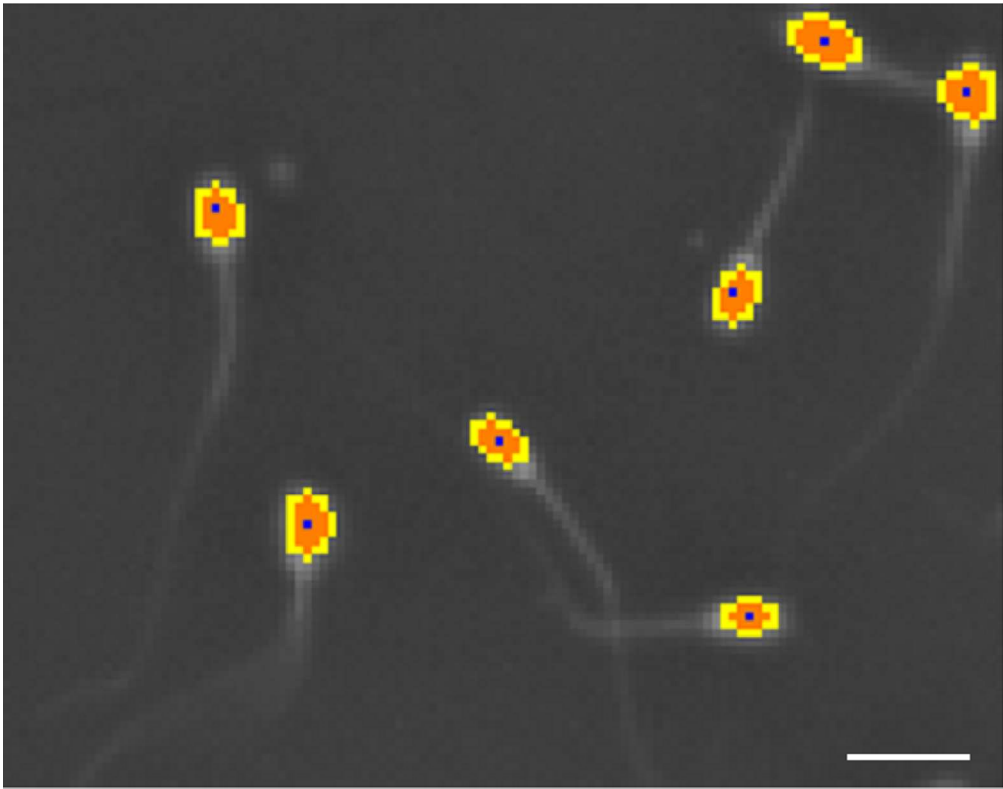


Figure 2: Zoom of a region with detected spermatozoa heads and their centroids. Bar= 10 μ m.

85x66mm (300 x 300 DPI)

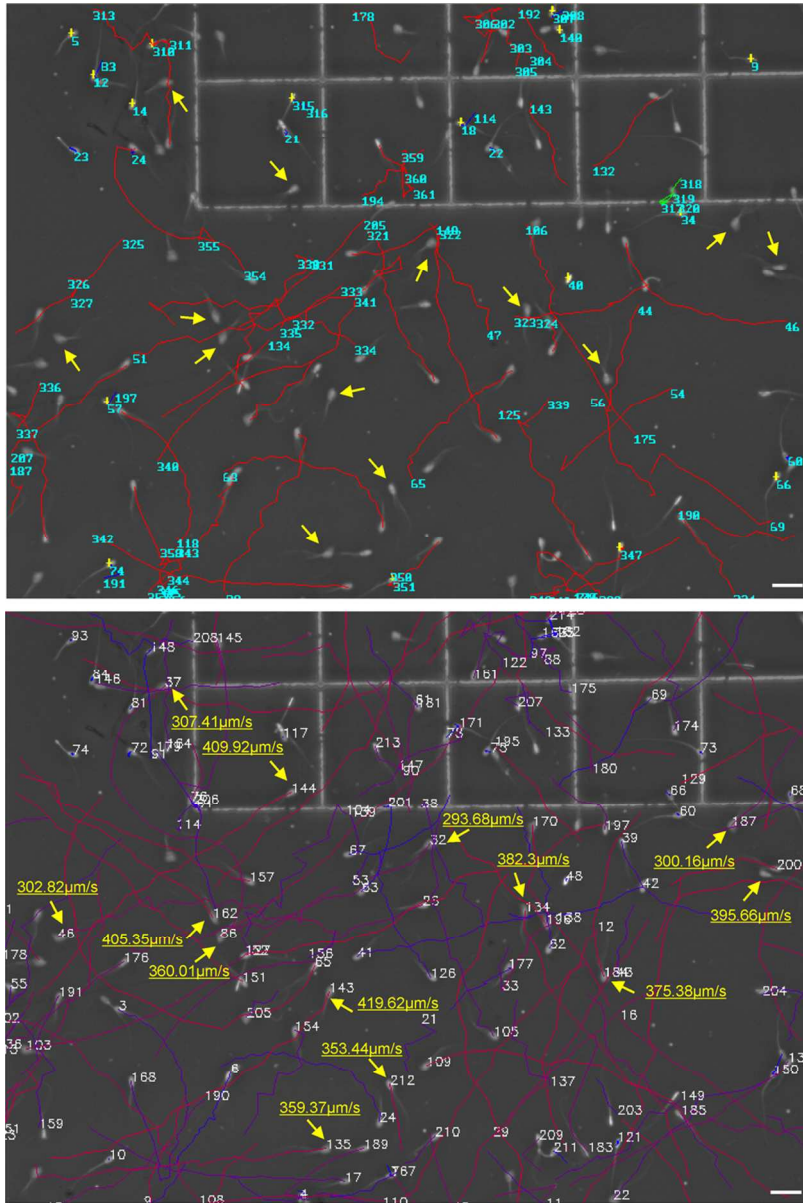


Figure 3: Visual comparison between trajectories detected by the SCA® versus the trajectories detected by the purposed sperm tracker software. The images correspond to the same video acquired at 25 fps (Video 5 of Table 2, <https://vimeo.com/264485794>), showing the totality of paths detected by the SCA® module (upper panel) or our tracker software (lower panel). Bar= 25 μm . Curvilinear Velocity (VCL, $\mu\text{m/s}$) of some sperm that were not detected with SCA® software (yellow arrows) are indicated with labels and arrows in the bottom panel corresponding to our software.

85x126mm (300 x 300 DPI)

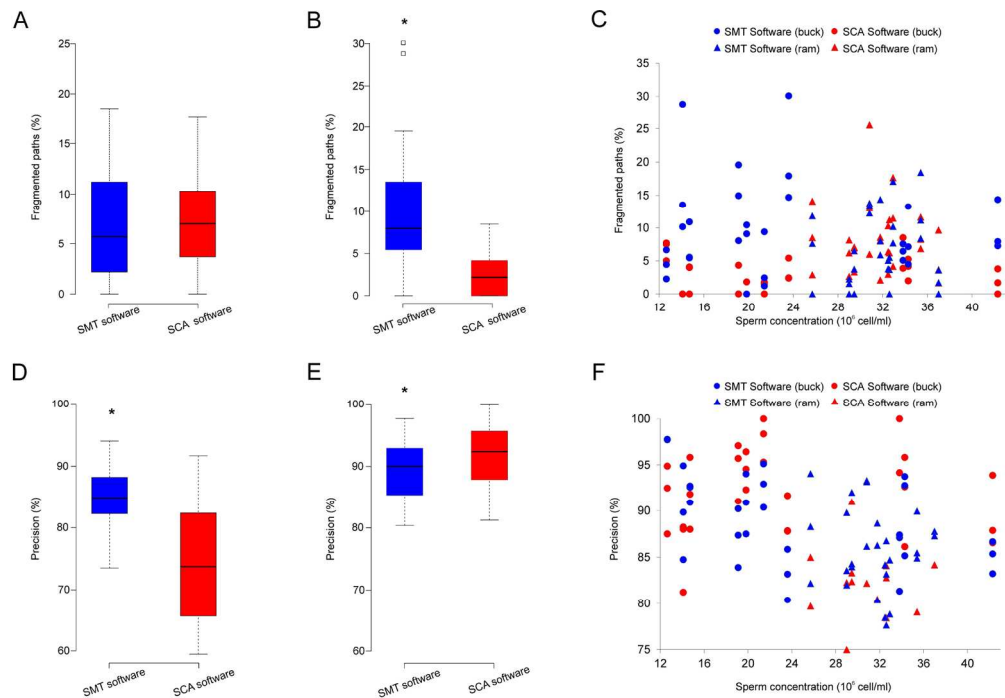


Figure 4: Performance of the sperm tracker software. Percentage of fragmented paths (A, B and C) or precision (D, E and F) for our Sperm tracker system (SMT software) compared to SCA® (SCA software) at 25 fps. Ram (A and D) or buck (B and E) sperm were analyzed. C and F panels gather results of all the analysis consider cell concentration as a variable. Data assemble the reports of three independent experts that analyzed 10 videos for each species. * Value significantly different with respect to SCA ®software ($p < 0.05$).

170x116mm (300 x 300 DPI)

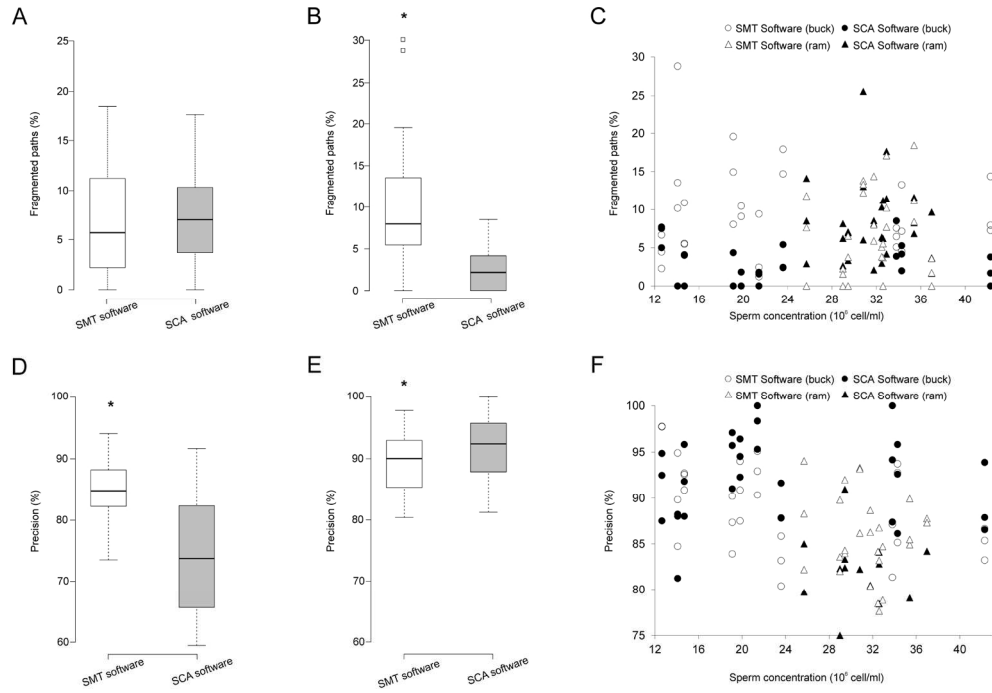


Figure 4: Performance of the sperm tracker software. Percentage of fragmented paths (A, B and C) or precision (D, E and F) for our Sperm tracker system (SMT software) compared to SCA® (SCA software) at 25 fps. Ram (A and D) or buck (B and E) sperm were analyzed. C and F panels gather results of all the analysis consider cell concentration as a variable. Data assemble the reports of three independent experts that analyzed 10 videos for each species. * Value significantly different with respect to SCA ®software (p< 0.05).

170x115mm (300 x 300 DPI)

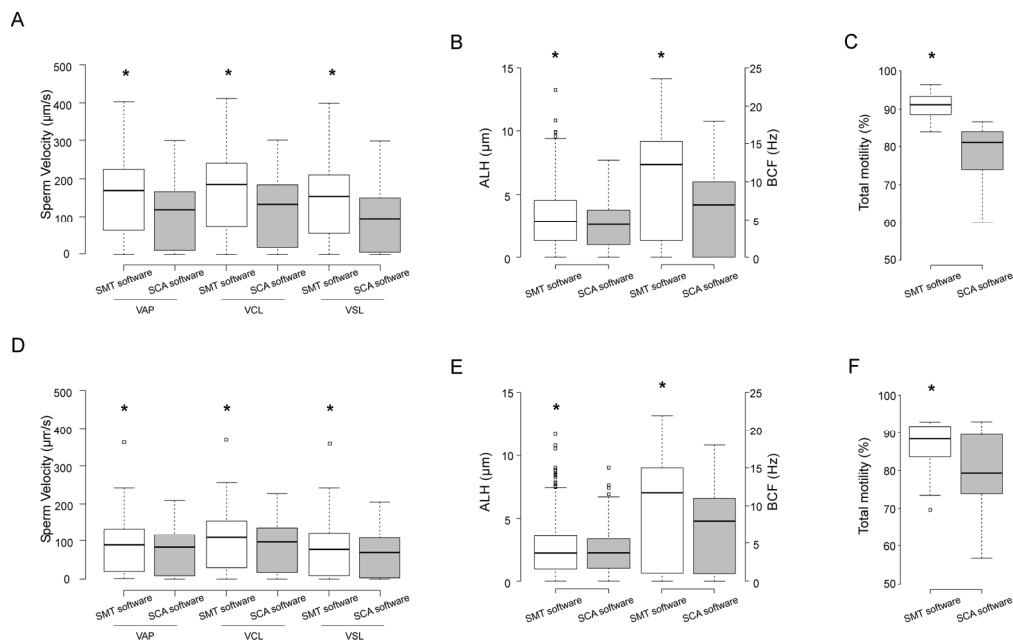


Figure 5: Report of Kinetic parameters analyzed by the commercial CASA system (SCA®) and the sperm motility tracker software (SMT) purposed by us. Sperm velocities: VAP, VSL and VCL (A and D), ALH and BCF (B and E) as well as total motility (C and F) were analyzed by both methods (SCA and SMT software) over the same samples. Analysis of ram samples are shown in A-C whereas analysis of buck samples are shown in D-E. . * Value significantly different with respect to SCA® software (p < 0.05). VAP: Average Path Velocity, VSL: Straight-Line Velocity, VCL: Curvilinear Velocity, ALH: Amplitude of Lateral Head Displacement, BCF: Beat Cross Frequency.

170x106mm (300 x 300 DPI)

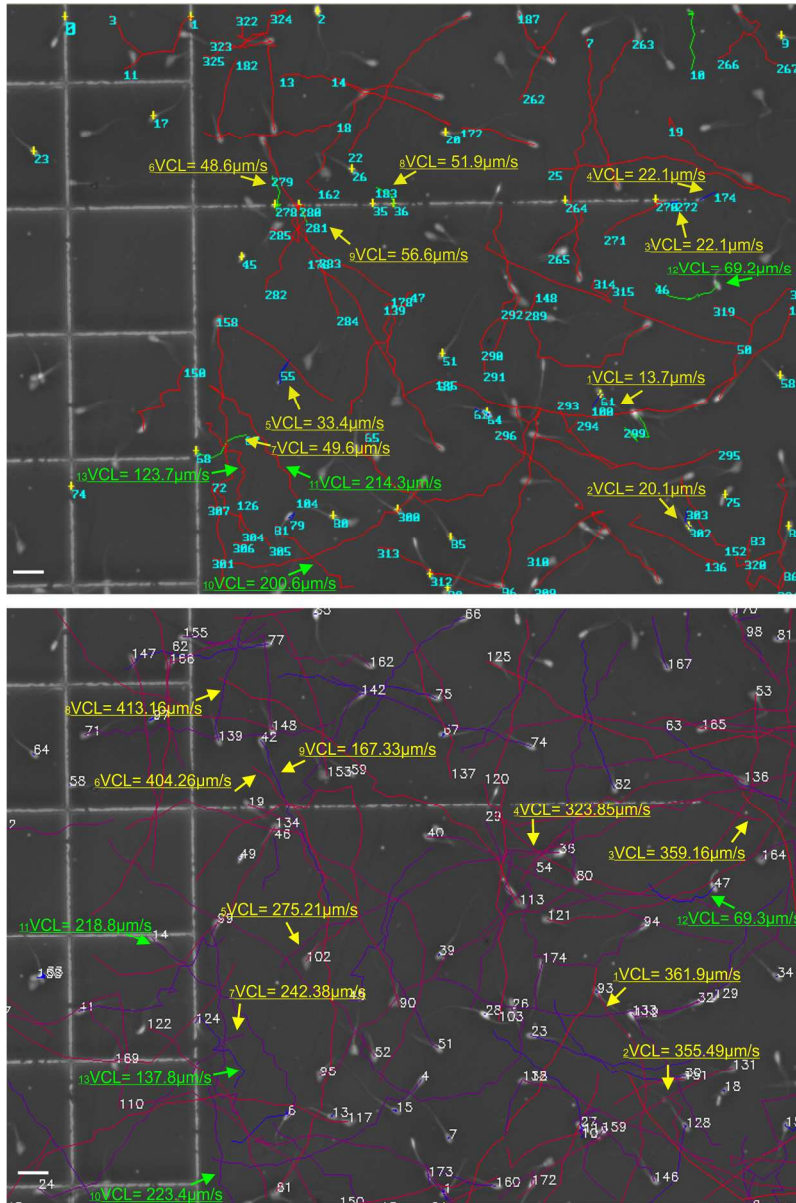


Figure 6: Visual comparison between trajectories detected by the SCA® (upper panel) versus the trajectories detected by the purposed sperm tracker software (bottom panel). The images correspond to the same video (Video 2 of Table 2, <https://vimeo.com/264482322>) acquired with 25 fps, showing the totality of paths detected with the SCA® module (upper panel) and our tracker software (bottom panel). Bar= 25 μm.

Curvilinear Velocities (VCL, μm/s) of some paths fragmented by SCA® software but tracked correctly by SMT are indicated with labels (1-9) and yellow arrows in the corresponding panels. Tracks with similar VCL (μm/s) comparing SMT to SCA® are indicated with labels (10-13) and green arrows in the corresponding panels.

170x256mm (300 x 300 DPI)

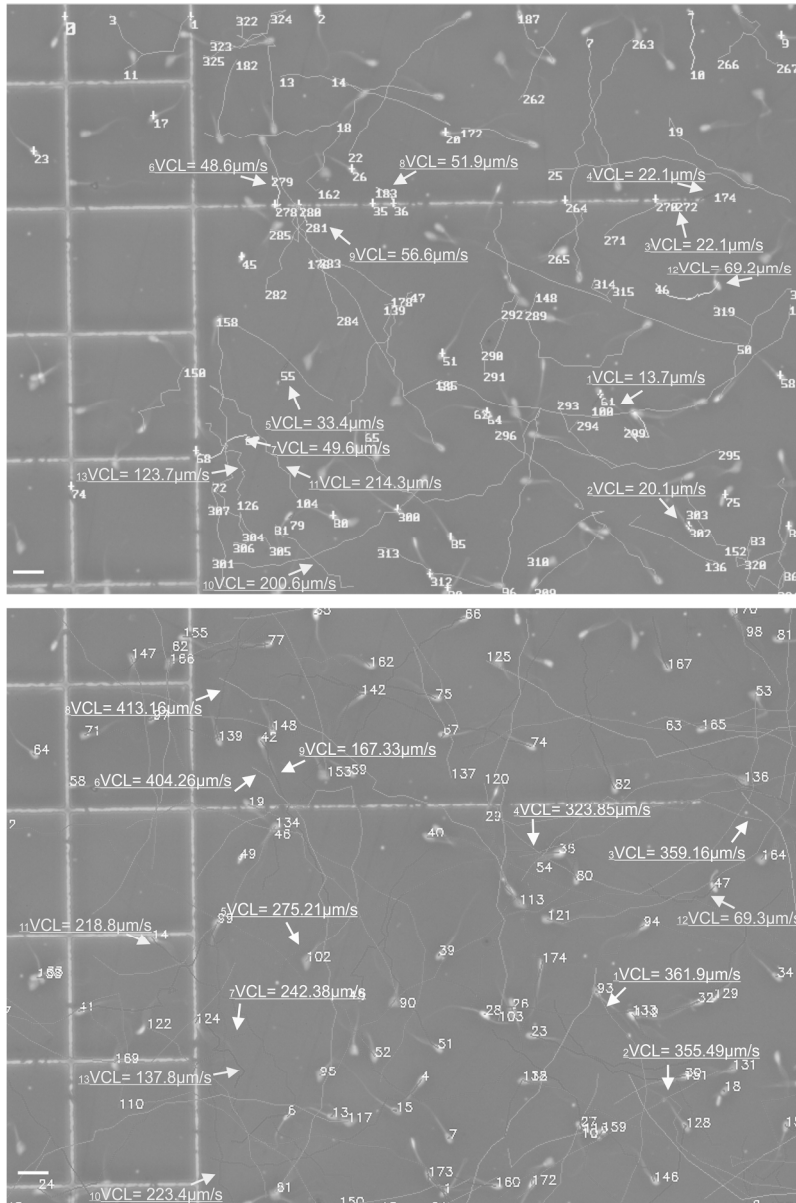


Figure 6: Visual comparison between trajectories detected by the SCA® (upper panel) versus the trajectories detected by the proposed sperm tracker software (bottom panel). The images correspond to the same video (Video 2 of Table 2, <https://vimeo.com/264482322>) acquired with 25 fps, showing the totality of paths detected with the SCA® module (upper panel) and our tracker software (bottom panel). Bar= 25 μm .

Curvilinear Velocities (VCL, $\mu\text{m/s}$) of some paths fragmented by SCA® software but tracked correctly by SMT are indicated with labels (1-9) and arrows in the corresponding panels. Tracks with similar VCL ($\mu\text{m/s}$) comparing SMT to SCA® are indicated with labels (10-13) and arrows in the corresponding panels.

170x256mm (300 x 300 DPI)

Table 1. Requirements for motility acquisition and analysis

Parameter	Characteristics
Chamber depth	10 μm
Maximum number of cells per field	≤ 120
Optimal sperm concentration	$\sim 35 \cdot 10^6$ cells/ml
Acquisition frame velocity with the camera	≥ 25 fps/sec*
Video recording time	5 sec
Microscope setting	Phase contrast, 10 x
Input to the software	Sequence of time-lapse images (MP4, AVI or MOV video)
System requirements to run software	I3 processor, 3 GB RAM, 1280x800 screen resolution.

* In this work, the kinetic values were compared between methods for 25 fps/sec due to camera limitations.

Table 2. Performance of the proposed tracker software (SMT) compared to SCA system

Animal	No video	Concentration (10 ⁶ cells/ml)	Software Proposed Method					SCA [®] system				
			% SCA tracks followed by SMT	Evaluated tracks \pm SE	% correctly detected particles (over total labelled particles)	Fragmented paths \pm SE (%)	Precision \pm SE (%)	Evaluated tracks \pm SE	% correctly detected particles (over total labelled particles)	Fragmented paths \pm SE (%)	Precision \pm SE (%)	
Ram	1	32.49	76.4 \pm 10.1	158 \pm 0	100 \pm 0.0	4.2 \pm 0.7	82.3 \pm 3.3	102 \pm 5	84.0 \pm 4.2	6.5 \pm 3.7	66.1 \pm 3.5	
	2	28.99	81.1 \pm 14.5	131 \pm 8	93.1 \pm 5.4	1.3 \pm 1.1	85.1 \pm 4.1	84 \pm 14	74.3 \pm 12.3	5.7 \pm 2.8	76.9 \pm 4.8	
	3	36.99	81.0 \pm 11.9	165 \pm 3	89.7 \pm 1.6	1.8 \pm 1.8	82.8 \pm 8.1	93 \pm 29	73.5 \pm 22.8	5.0 \pm 4.2	74.3 \pm 8.9	
	4	32.60	78.2 \pm 14.2	155 \pm 19	88.4 \pm 10.6	3.1 \pm 2.8	82.5 \pm 4.6	84 \pm 30	64.9 \pm 23.0	5.8 \pm 5.6	81.8 \pm 3.0	
	5	29.45	83.6 \pm 9.8	151 \pm 11	89.9 \pm 6.8	3.4 \pm 3.3	86.8 \pm 4.6	72 \pm 14	71.6 \pm 13.5	5.8 \pm 2.1	85.9 \pm 4.8	
	6	35.40	79.4 \pm 1.3	179 \pm 1	99.6 \pm 0.3	12.7 \pm 5.2	86.8 \pm 2.8	108 \pm 19	82.2 \pm 14.4	8.9 \pm 2.5	69.2 \pm 9.6	
	7	31.80	74.3 \pm 3.5	152 \pm 2	98.7 \pm 1.1	9.4 \pm 4.4	85.1 \pm 4.3	95 \pm 14	79.4 \pm 11.7	6.2 \pm 3.6	67.8 \pm 11.2	
	8	32.92	82.0 \pm 4.9	157 \pm 1	98.1 \pm 0.6	11.7 \pm 4.9	79.4 \pm 5.0	92 \pm 6	76.0 \pm 5.0	11.1 \pm 6.7	69.1 \pm 3.7	

	9	30.82	80.9 ± 2.4	150 ± 3	98.5 ± 1.7	13.1 ± 0.8	90.9 ± 4.1	99 ± 11	82.9 ± 9.3	14.9 ± 9.9	68.0 ± 12.4
	10	25.70	88.4 ± 10.7	118 ± 3	85.3 ± 1.8	6.5 ± 6.0	88.2 ± 5.9	74 ± 4	78.7 ± 4.6	8.5 ± 5.6	79.6 ± 5.5
Buck	1	19.82	98.2 ± 0.1	65 ± 2	82.7 ± 2.6	6.5 ± 5.7	90.8 ± 3.3	54 ± 2	92.1 ± 3.5	0.6 ± 1.0	94.4 ± 2.1
	2	21.41	99.5 ± 0.9	83 ± 2	96.51 ± 2.0	4.4 ± 4.4	92.8 ± 2.4	60 ± 4	90.0 ± 6.0	1.1 ± 1.0	97.9 ± 2.4
	3	42.29	97.1 ± 0.3	165 ± 2	98.2 ± 1.2	9.9 ± 3.9	85.1 ± 1.7	127 ± 7	92.0 ± 5.1	1.8 ± 1.9	89.4 ± 3.9
	4	33.81	97.1 ± 0.9	123 ± 6	93.2 ± 4.2	6.4 ± 1.2	85.3 ± 3.4	102 ± 2	96.8 ± 2.2	5.4 ± 2.7	93.9 ± 6.3
	5	34.28	99.3 ± 1.1	114 ± 5	93.2 ± 3.9	8.3 ± 4.5	90.6 ± 4.7	97 ± 4	92.9 ± 3.9	3.8 ± 1.7	91.5 ± 4.9
	6	12.64	100 ± 0.0	44 ± 1	98.5 ± 1.3	4.5 ± 2.2	97.8 ± 0.0	40 ± 1	96.7 ± 1.4	6.7 ± 1.5	91.6 ± 3.8
	7	14.7	95.2 ± 1.3	54 ± 1	98.8 ± 1.0	7.3 ± 3.1	92.1 ± 1.0	49 ± 1	94.2 ± 1.9	2.7 ± 2.3	91.9 ± 3.9
	8	14.09	95.3 ± 1.1	59 ± 1	99.4 ± 1.0	17.5 ± 9.9	89.8 ± 5.1	50 ± 2	92.0 ± 2.8	0.0 ± 0.0	85.8 ± 4.0
	9	19.1	97.1 ± 2.6	88 ± 3	93.4 ± 3.4	14.2 ± 5.8	87.2 ± 3.2	69 ± 2	95.4 ± 2.1	1.4 ± 2.5	94.6 ± 3.2
	10	23.59	97.5 ± 1.1	107 ± 6	93.6 ± 5.3	20.9 ± 8.1	83.1 ± 2.7	80 ± 6	89.5 ± 6.6	3.4 ± 1.7	89.1 ± 2.2